

SUPPLEMENTARY INFORMATION for

Surface and volume energies of α -, β -, and κ -Ga₂O₃ under epitaxial strain induced by a sapphire substrate

Ilaria Bertoni, Aldo Ugolotti, Emilio Scalise and Leo Miglio

Department of Materials Science, Università degli Studi di Milano-Bicocca, via Cozzi 55 I-20125 Milano, Italy

Comparison of structural properties and cohesive energies calculated with different exchange and correlation functionals, along with the corresponding values reported in literature; valence charges calculated by the Bader criterion.

We report in Table S1 the structural parameters and the corresponding cohesive energy E_{coh} for the β (monoclinic), the κ (orthorhombic), and the α (rhombohedral) phases of Ga₂O₃, as calculated with different exchange and correlation functionals, and their comparison with the results reported in the literature. There is an overall agreement between AM05, PBEsol and SCAN results, while the PBE values stand out because of the larger differences between the calculated energies of the different polymorphs. Analogously, the lattice parameters optimized through the AM05, PBEsol and SCAN functional are in good agreement with the experimental values, while the results for PBE are larger than those calculated with other functionals. Focusing on the hierarchy in E_{coh} among the different phases, the β polymorph is always the most stable one, as expected. However, the order of the other two phases is not always the same in the case of the PBE and the AM05 functionals, the κ polymorph is more stable than the α one, while the SCAN and the PBEsol agree to reverse the order. Still, the differences in E_{coh} are as low as few meV/atom and we selected PBEsol to be the closest cost-efficient method to the reliable SCAN prediction.

In Table S2 we report the comparison between the Bader charges^(1,2) calculated with different functionals, using a cutoff of 500 eV, within the structural configurations predicted by the PBEsol exchange and correlation (xc) functional. There is an overall agreement of the values calculated with the different functionals, with the SCAN results showing a slightly more ionic character. The charge partitioning is very similar among the different Ga₂O₃ phases.

Phase	xc functional	$\Delta E_{\text{coh}}^{\beta}$ (meV/atom)	ρ (atoms \AA^{-3})	a (\AA)	b (\AA)	c (\AA)	angle ($^{\circ}$)
β	PBE	0.0	0.091	12.46 [12.44 ⁽³⁾]	3.09 [3.08 ⁽³⁾]	5.88 [5.88 ⁽³⁾]	103.6 [103.7 ⁽³⁾]
	AM05		0.095	12.30 [12.29 ⁽⁴⁾]	3.05 [3.05 ⁽⁴⁾]	5.81 [5.81 ⁽⁴⁾]	103.7 [103.8 ⁽⁴⁾]
	SCAN		0.095	12.25	3.04	5.82	103.8
	PBEsol		0.095	12.28	3.05	5.81	103.7
	expt.	-	0.095 ⁽⁵⁾	12.2 ⁽⁵⁾	3.04 ⁽⁵⁾	5.81 ⁽⁵⁾	103.8 ⁽⁵⁾
κ	PBE	20.0 [20 ⁽⁶⁾]	0.095	5.12	8.80	9.42	90.0
	AM05	16.3 [16.2 ⁽⁴⁾]	0.098	5.06 [5.06 ⁽⁴⁾]	8.69 [8.69 ⁽⁴⁾]	9.30 [9.30 ⁽⁴⁾]	90.0
	SCAN	14.4 [15 ⁽⁶⁾]	0.098	5.05	8.68	9.28	90.0
	PBEsol	12.6 [13 ⁽⁶⁾]	0.098	5.06	8.69	9.29	90.0
	expt.	-	0.098 ⁽⁷⁾	5.05 ⁽⁷⁾	8.70 ⁽⁷⁾	9.28 ⁽⁷⁾	90.0
α	PBE	27.1 [28 ⁽⁶⁾]	0.100	5.06 [5.06 ⁽³⁾]		13.61 [13.62 ⁽³⁾]	60.0
	AM05	17.2 [17.8 ⁽⁴⁾]	0.103	5.00 [5.00 ⁽⁴⁾]		13.46 [13.45 ⁽⁴⁾]	60.0
	SCAN	12.0 [10 ⁽⁶⁾]	0.104	4.98		13.45	60.0
	PBEsol	9.1 [9 ⁽⁶⁾]	0.103	5.00		13.45	60.0
	expt.	-	0.103 ⁽⁵⁾	4.98 ⁽⁵⁾		13.43 ⁽⁵⁾	60.0

Table S1: comparison of bulk cohesive energies E_{coh} referred to the most stable β polymorph ($\Delta E_{\text{coh}}^{\beta}$) and structural parameters (atomic density ρ , lattice parameters, and unit vector angle) calculated with different exchange and correlation (xc) functionals. The crystal cell structures were optimized with an enlarged plane-waves cutoff of 850 eV; then E_{coh} was calculated with the default cutoff of 500 eV.

xc functional	α		β			κ		
	Ga _{oct}	O	Ga _{oct}	Ga _{tetra}	O _{min/max}	Ga _{oct}	Ga _{tetra}	O _{min/max}
PBE	11.13	7.25	11.10	11.17	7.23/7.24	11.12	11.16	7.23/7.27
PBEsol	11.15	7.23	11.12	11.19	7.22/7.24	11.14	11.18	7.22/7.26
AM05	11.13	7.25	11.11	11.18	7.23/7.25	11.13	11.17	7.22/7.26
SCAN	11.04	7.30	11.03	11.10	7.28/7.30	11.04	11.10	7.28/7.32

Table S2: Bader valence charges (e⁻) calculated for the bulk of different Ga₂O₃ polymorphs. As a reference, the valence states of the isolated Ga or O atoms have 13 and 6 electrons, respectively.

Additional details about the surface structure of Ga₂O₃ polymorphs: in-plane unit cells, simultaneous equation method, and comparison among the structures and the atomic coordinations of the as-cut, relaxed and reconstructed surfaces of all slabs.

In Table S3 we report the cell parameters of our slab configurations, for different surface orientations and phases: both the primitive and the conventional unit cells are reported, along with the values already reported in the literature. Since we want to deal with (ideally) non-interacting slabs rather than slabs stacked as heterostructures, along the direction perpendicular to the surface the only important parameter is the distance between one slab and its (fictitious) replica, which we recall is at least 13 Å. Therefore, we report only the in-plane unit cell of the slab. As a reference, we also report the in-plane unit cell of our (0001) α -Al₂O₃ surface obtained from the bulk structure we optimized including the Al pseudopotential with 3 valence electrons, an energy cutoff of 850 eV and a 5x5x5 k-point grid.

In the case of the κ -Ga₂O₃ {001}, the two opposite surfaces are not equivalent since this slab doesn't possess mirror symmetry. Hence, the surface energy γ calculated through the linear extrapolation method⁽⁶⁾ would correspond to the average between the actual γ of the (001) and (00-1) surfaces. In order to decouple these two contributions, we followed the approach described in ref. (8), called "simultaneous equation method", where we consider four variables, i.e. the surface energy of the two terminations when their coordinates are fixed or optimized as $\gamma_{(001)}^{fixed}$, $\gamma_{(00-1)}^{fixed}$, $\gamma_{(001)}^{relaxed}$ and $\gamma_{(00-1)}^{relaxed}$, the values of which we want to obtain. Since we can selectively fix or optimize one surface and/or the other, we obtain four average surface energies Γ_{1-4} that can be related to the individual surface energies through the following set of equations:

$$\begin{aligned} \gamma_{(001)}^{fixed} + \gamma_{(00-1)}^{fixed} &= \Gamma_1 \\ \gamma_{(001)}^{fixed} + \gamma_{(00-1)}^{relaxed} &= \Gamma_2 \\ \gamma_{(001)}^{relaxed} + \gamma_{(00-1)}^{fixed} &= \Gamma_3 \\ \gamma_{(001)}^{relaxed} + \gamma_{(00-1)}^{relaxed} &= \Gamma_4 \end{aligned}$$

i.e. $A\vec{\gamma} = \vec{\Gamma}$

Such a system cannot be trivially solved since the matrix of the coefficients is singular. Therefore, we sought an approximated numerical solution, by replacing $\vec{\Gamma}$ with $\vec{\Gamma} + \vec{r}$, i.e. introducing the vector \vec{r} of residuals and minimizing its square modulus. Therefore, we followed an iterative algorithm where at any step i the residuals are calculated as $\vec{r}^i = A\vec{\gamma}^i - \vec{\Gamma}$ and the next iteration is performed by changing the guess surface energies as $\vec{\gamma}^{i+1} = \vec{\gamma}^i + \vec{\epsilon}^i$, where the step $\vec{\epsilon}^{i+1} = \nabla_{\vec{\gamma}}\vec{r}$ is determined through the steepest descent approach.

Indeed, our method cannot guarantee to identify the global minimum of the residual function, as the choice of the initial guess is critical. We initialized our algorithm assuming equal surface energies for the (001) and the (00-1) surfaces, with values calculated from slabs of different thickness with optimized or with fixed coordinates. We made this choice because the analysis of the coordination environment of the Ga atoms at the surface, showing differences just in the sub-surface region (see Figure S9 and S10 below), suggests only minor differences in the surface energies of the two terminations.

In Figure S1-S10 we report the geometry of the surface region of all the slabs included in our investigation, where we also highlight the major atomic displacements from one optimization step to the following. In addition, in each figure, we show the comparison of the pair distribution function calculated for selected Ga atoms in the unstrained bulk and at the surface of the unstrained slabs. We highlight these atoms within each image and label them for example as “Ga 1” or “Ga 2”, etc. For the Ga atoms closest to the surface, we report directly in the structure the average number of first neighbors, calculated integrating the pair distribution function up to 2.5 Å.

Phase-surface		Type of in-plane cell	a (Å)	b (Å)	a∧b (°)
β-Ga ₂ O ₃	(-201)	primitive	3.048 [3.07 ⁽⁹⁾]	7.536 [7.59 ⁽⁹⁾]	78.3 [78.3 ⁽⁹⁾]
		conventional	3.048 [3.05 ^{(5)*}]	14.761 [14.705 ^{(5)*}]	90.0
	(11-2)	primitive	6.325 [6.36 ⁽⁹⁾]	8.682 [8.75 ⁽⁹⁾]	113.87 [113.8 ⁽⁹⁾]
	(100)	primitive	3.048 [3.07 ⁽⁹⁾]	5.813 [5.86 ⁽⁹⁾]	90.00 [90.0 ⁽⁹⁾]
κ-Ga ₂ O ₃	{001}	primitive	5.061	8.685	90.00
	(100)	primitive	8.685	9.293	90.00
	(010)	primitive	5.061	9.293	90.00
α-Ga ₂ O ₃	(001)	primitive	5.001 [10.065 ^{(10)**}]		60.00 [60.00 ⁽¹⁰⁾]
		conventional	5.001	8.660	90.0
	(100)	conventional ⁺	13.443 [13.504 ⁽¹⁰⁾]	5.001 [5.032 ⁽¹⁰⁾]	90.00 [90.00 ⁽¹⁰⁾]
	(012)	primitive	5.001 [5.032 ^{(10)***}]	7.315 [16.072 ^{(10)***}]	46.80 [90.00 ^{(10)***}]
α-Al ₂ O ₃	(001)	primitive	4.805 [4.756 ⁽¹¹⁾]		120.0
		conventional	4.805	8.323 [8.238 ^{(11)****}]	90.0

Table S3: comparison of our calculated in-plane crystal structures of different Ga₂O₃ and Al₂O₃ surfaces with the values available in the literature.

⁺: supercell not unitary

^{*}: calculated from the reported bulk

^{**}: for the 2x2 supercell

^{***}: conventional cell

^{****}: calculated from the reported primitive.

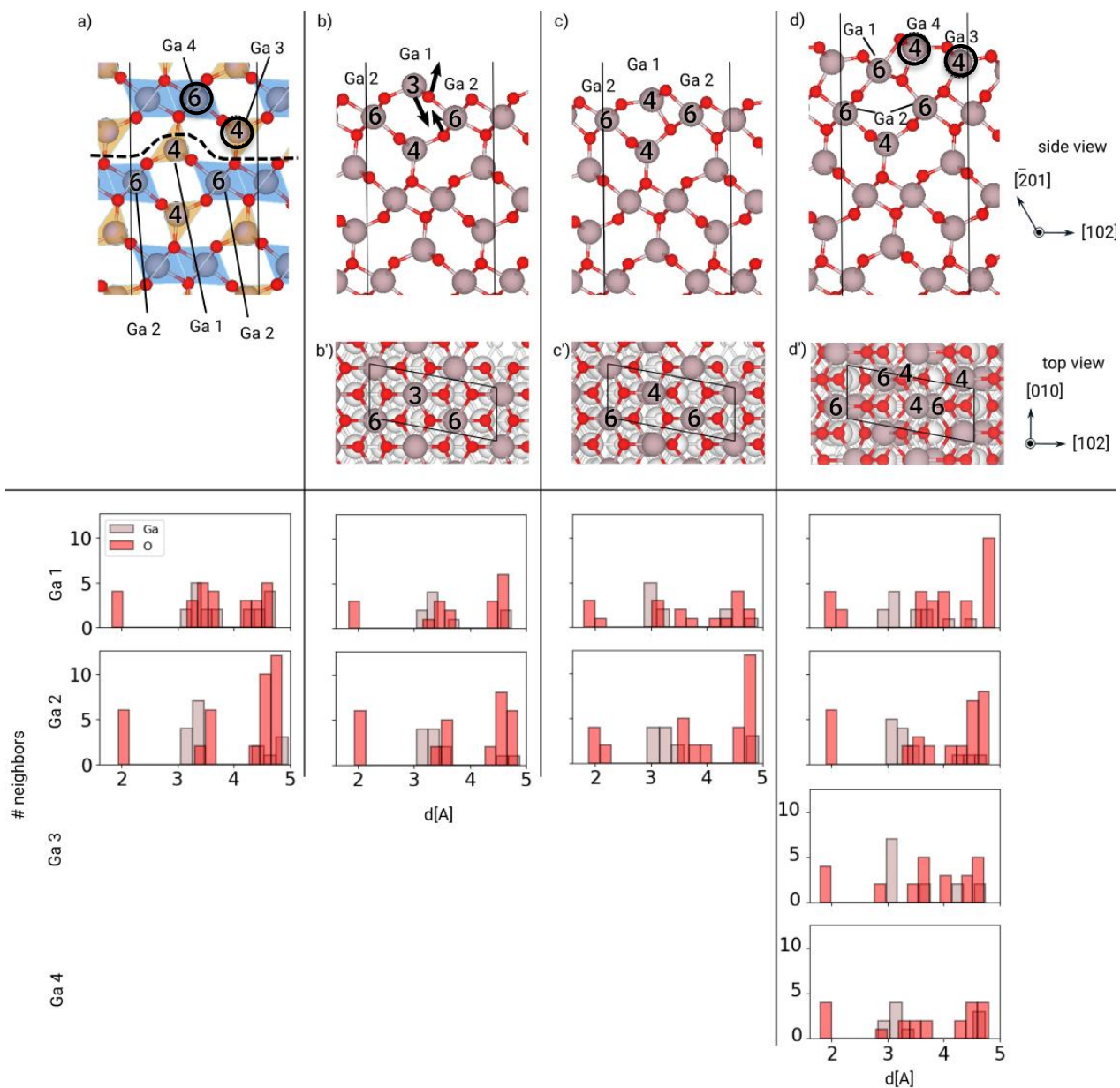


Figure S1: structure (upper panels) and pair distribution function (lower panels) of the slab of the (-201) surface of β - Ga_2O_3 at different steps of optimization: (a) bulk, (b-b') "as-cut", (c-c') "relaxed" and (d-d') "reconstructed". In the case of the bulk, the different tetrahedral or octahedral cages are represented through orange or blue polyhedra, respectively. The most important atomic displacements between one structure and the following are highlighted by black arrows. For the atoms closest to the surface, the average number of first neighbors is reported. For the sake of clarity, out of the two full formula units added to the "relaxed" geometry in order to obtain the "reconstructed" one, in panel a and d we mark by black circles the two Ga atoms only. The interatomic distances are shown for selected Ga atoms, labelled "Ga 1", "Ga 2", "Ga 3" and "Ga 4".

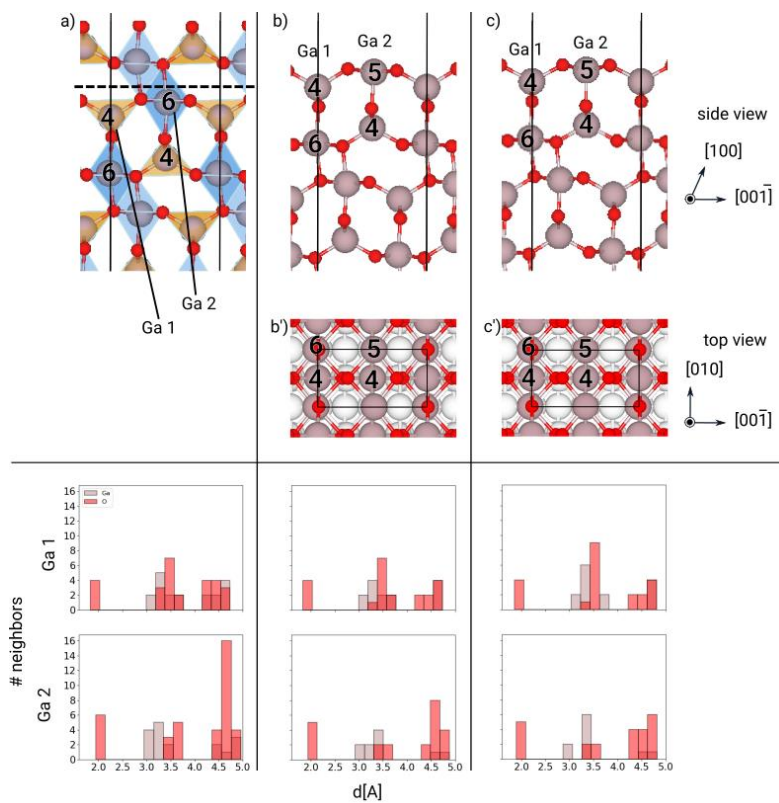


Figure S2: structure (upper panels) and pair distribution function (lower panels) of the slab of the (100) surface of β - Ga_2O_3 at different steps of optimization: (a) bulk, (b-b') "as-cut" and (c-c') "relaxed". In the case of the bulk, the different tetrahedral or octahedral cages are represented through orange or blue polyhedra, respectively. The most important atomic displacements between one structure and the following are highlighted by black arrows. For the atoms closest to the surface, the average number of first neighbors is reported. The interatomic distances are shown for selected Ga atoms, labelled "Ga 1" and "Ga 2".

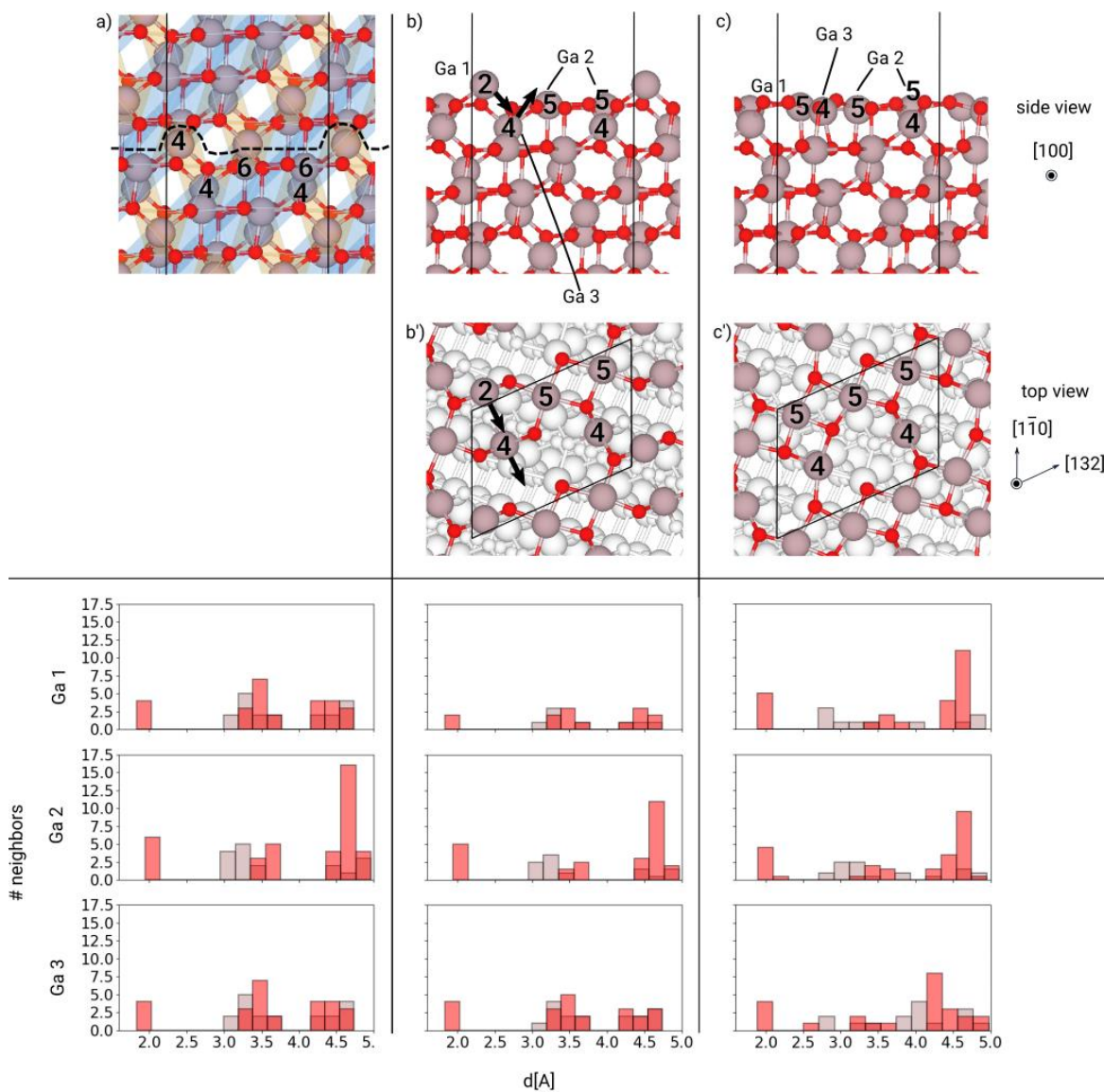


Figure S3: structure (upper panels) and pair distribution function (lower panels) of the slab of the (11-2) surface of β - Ga_2O_3 at different steps of optimization: (a) bulk, (b-b') "as-cut" and (c-c') "relaxed". In the case of the bulk, the different tetrahedral or octahedral cages are represented through orange or blue polyhedra, respectively. For the atoms closest to the surface, the average number of first neighbors is reported. The most important atomic displacements between one structure and the following are highlighted by black arrows. The interatomic distances are shown for selected Ga atoms, labelled "Ga 1", "Ga 2" and "Ga 3".

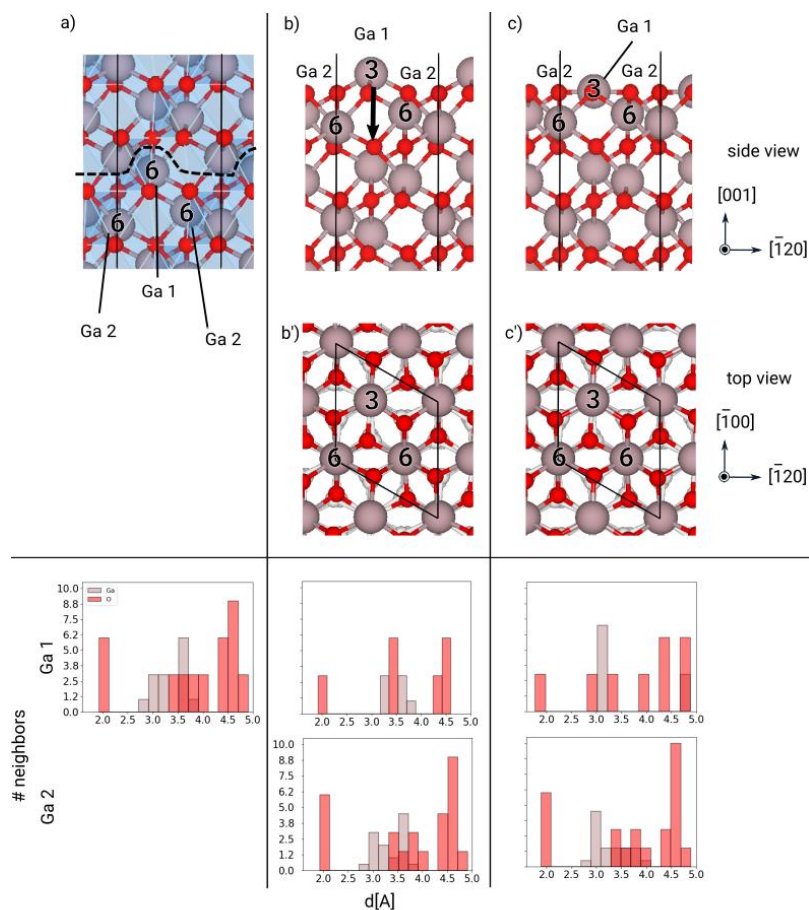


Figure S4: structure (upper panels) and pair distribution function (lower panels) of the slab of the (001) surface of α - Ga_2O_3 at different steps of optimization: (a) bulk, (b-b') "as-cut" and (c-c') "relaxed". In the case of the bulk, the octahedral cages are represented through blue polyhedra. For the atoms closest to the surface, the average number of first neighbors is reported. The most important atomic displacements between one structure and the following are highlighted by black arrows. The interatomic distances are shown for selected Ga atoms; the surface Ga atoms (labelled "Ga 1") have a different coordination than all bulk ones (labelled "Ga 2").

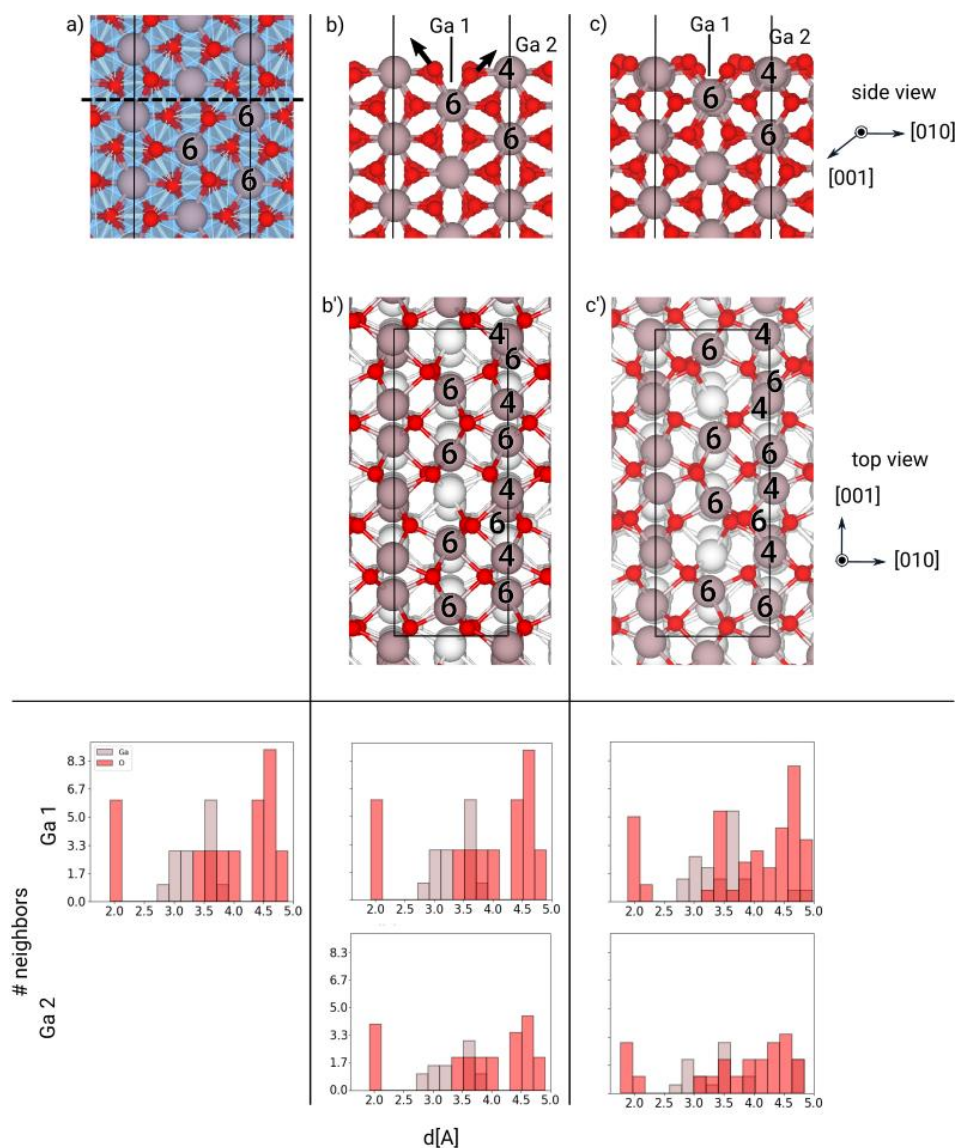


Figure S5: structure (upper panels) and pair distribution function (lower panels) of the slab of the (100) surface of α - Ga_2O_3 at different steps of optimization: (a) bulk, (b-b') "as-cut" and (c-c') "relaxed". In the case of the bulk, the octahedral cages are represented through blue polyhedra. For the atoms closest to the surface, the average number of first neighbors is reported. The most important atomic displacements between one structure and the following are highlighted by black arrows. The interatomic distances are shown for selected Ga atoms; the surface Ga atoms (labelled "Ga 1") have a different coordination than all bulk ones (labelled "Ga 2").

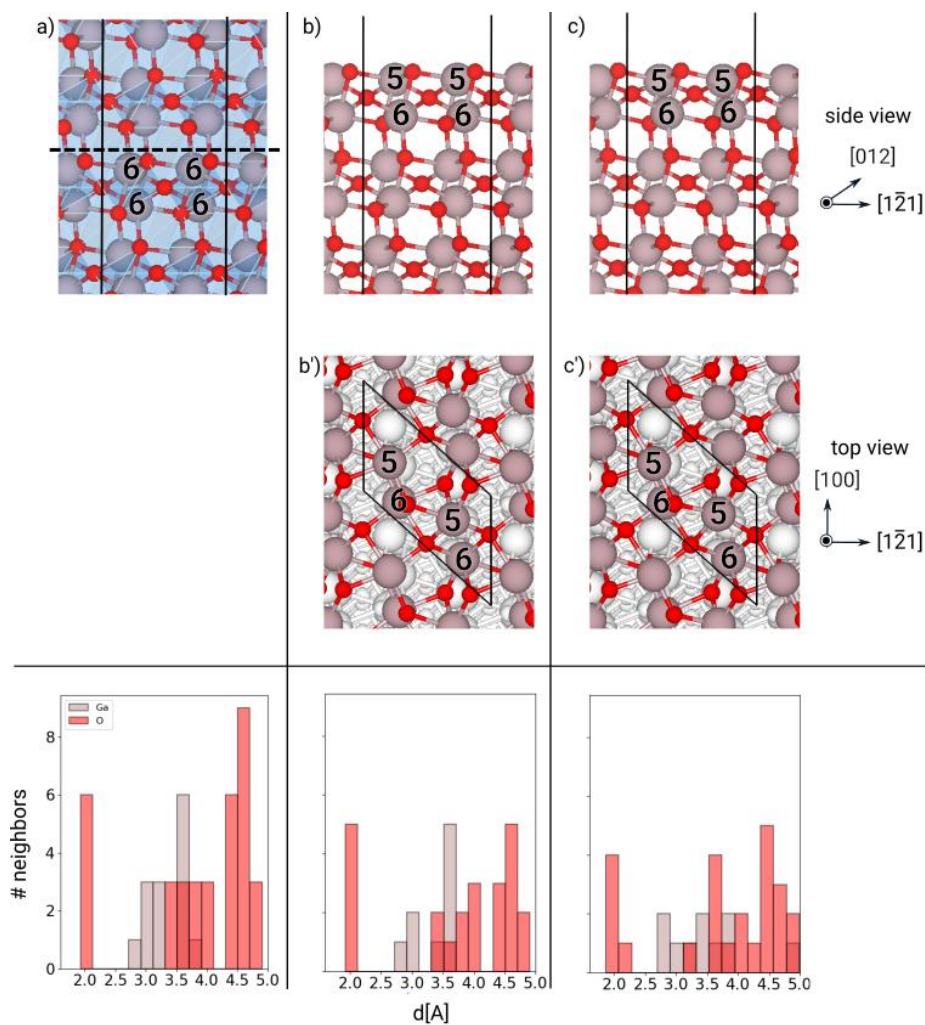


Figure S6: structure (upper panels) and pair distribution function (lower panels) of the slab of the (012) surface of α - Ga_2O_3 at different steps of optimization: (a) bulk, (b-b') "as-cut" and (c-c') "relaxed". In the case of the bulk, the octahedral cages are represented through polyhedra, respectively. For the atoms closest to the surface, the average number of first neighbors is reported. The most important atomic displacements between one structure and the following are highlighted by black arrows. The interatomic distances are shown for the topmost Ga atom in panel b and c, while those of the bulk atoms are reported for comparison below panel a.

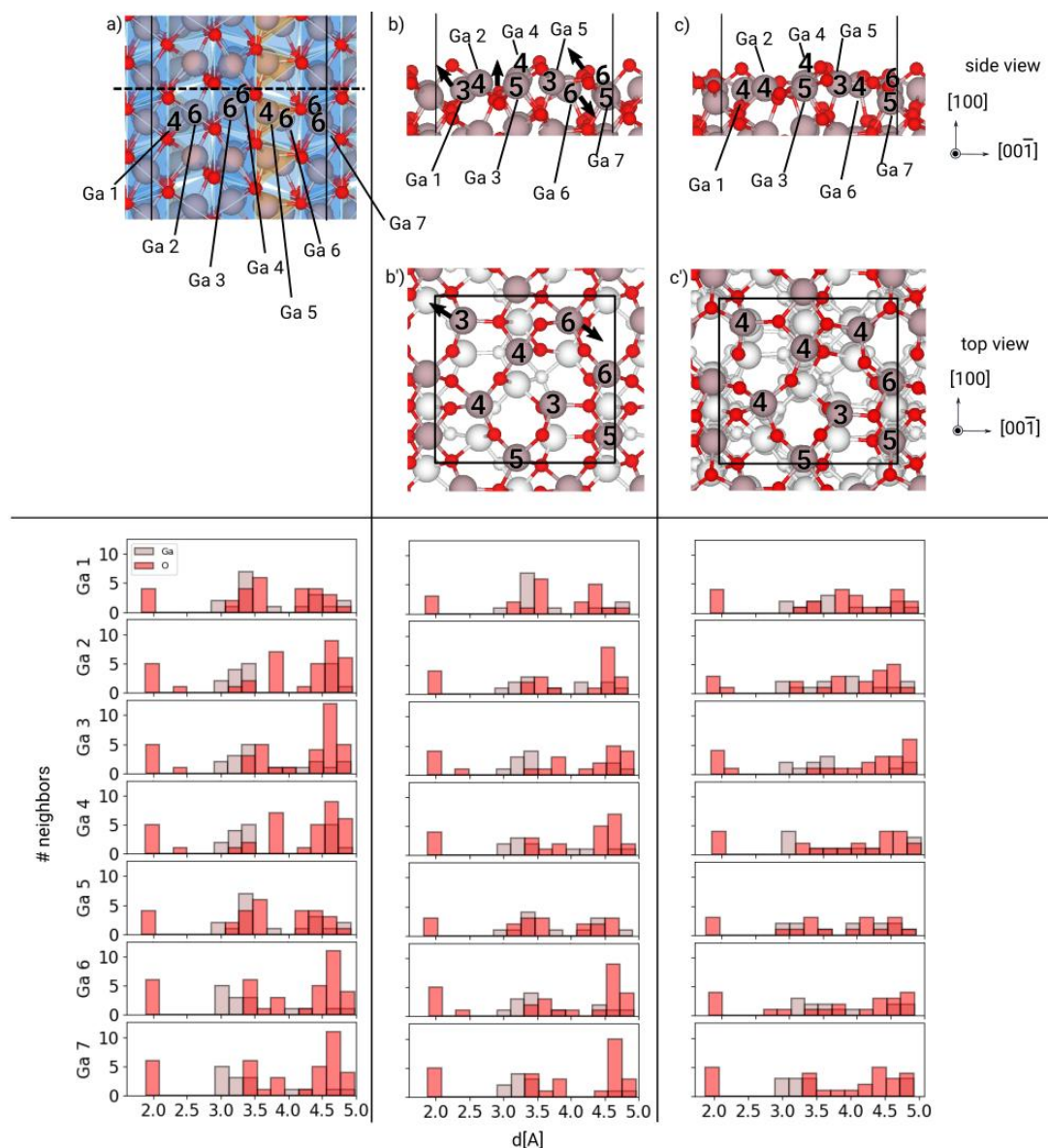


Figure S7: structure (upper panels) and pair distribution function (lower panels) of the slab of the (100) surface of κ -Ga₂O₃ at different steps of optimization: (a) bulk, (b-b') "as-cut" and (c-c') "relaxed". In the case of the bulk, the different tetrahedral or octahedral cages are represented through orange or blue polyhedra, respectively. For the atoms closest to the surface, the average number of first neighbors is reported. The most important atomic displacements between one structure and the following are highlighted by black arrows. The interatomic distances are shown for selected Ga atoms, labelled "Ga 1", "Ga 2", "Ga 3", "Ga 4" and "Ga 5".

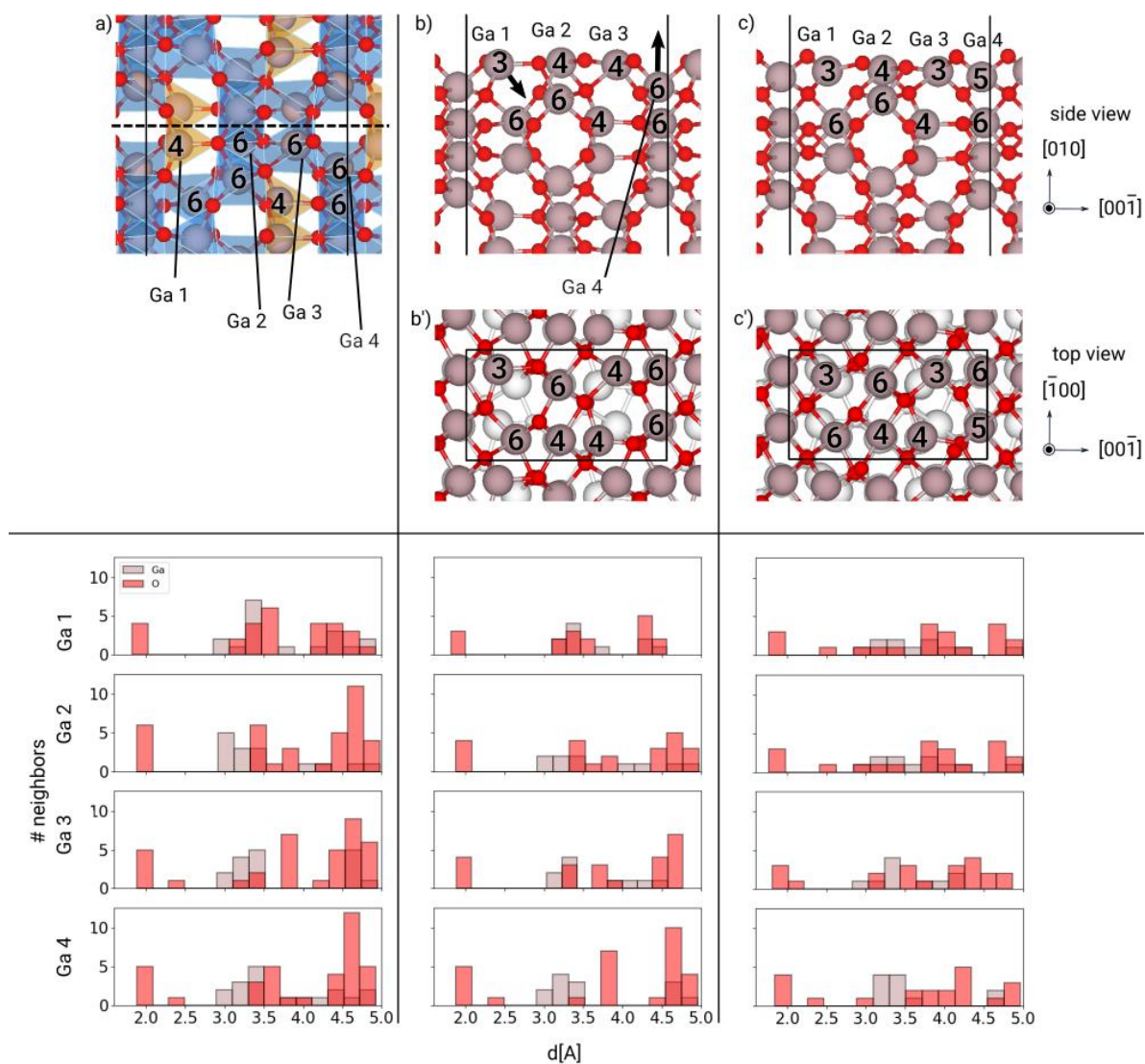


Figure S8: structure (upper panels) and pair distribution function (lower panels) of the slab of the (010) surface of κ - Ga_2O_3 at different steps of optimization: (a) bulk, (b-b') "as-cut" and (c-c') "relaxed". In the case of the bulk, the different tetrahedral or octahedral cages are represented through orange or blue polyhedra, respectively. For the atoms closest to the surface, the average number of first neighbors is reported. The most important atomic displacements between one structure and the following are highlighted by black arrows. The interatomic distances are shown for selected Ga atoms, labelled "Ga 1", "Ga 2", "Ga 3" and "Ga 4".

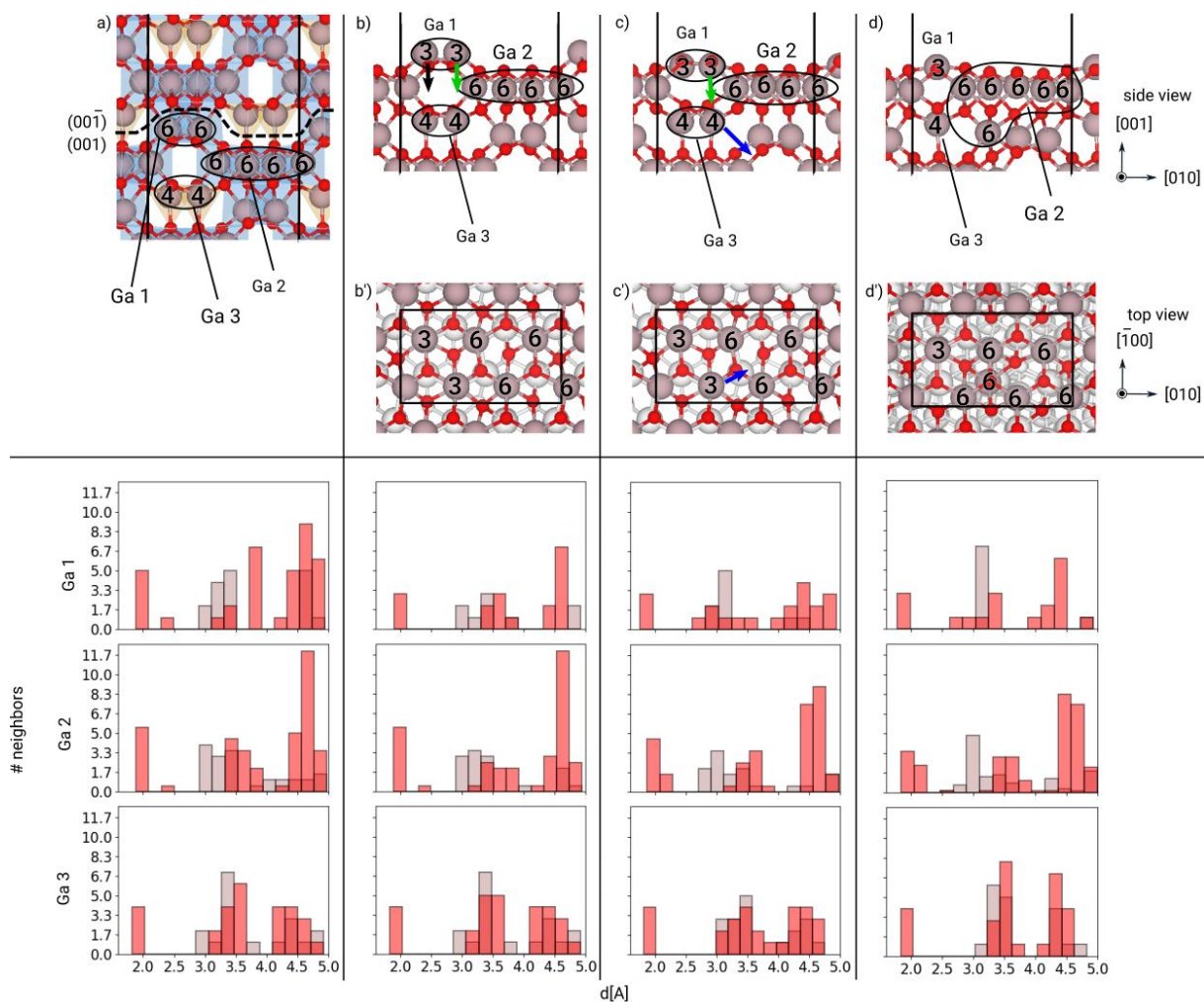


Figure S9: structure (upper panels) and pair distribution function (lower panels) of the slab of the (001) surface of κ - Ga_2O_3 at different steps of optimization: (a) bulk, (b-b') "as-cut", (c-c') "relaxed" and (d-d') "reconstructed". In the case of the bulk, the different tetrahedral or octahedral cages are represented through orange or blue polyhedra, respectively. For the atoms closest to the surface, the average number of first neighbors is reported. The most important atomic displacements between one structure and the following are highlighted by black, blue and green arrows. The interatomic distances are shown for selected Ga atoms, labelled "Ga 1", "Ga 2" and "Ga 3".

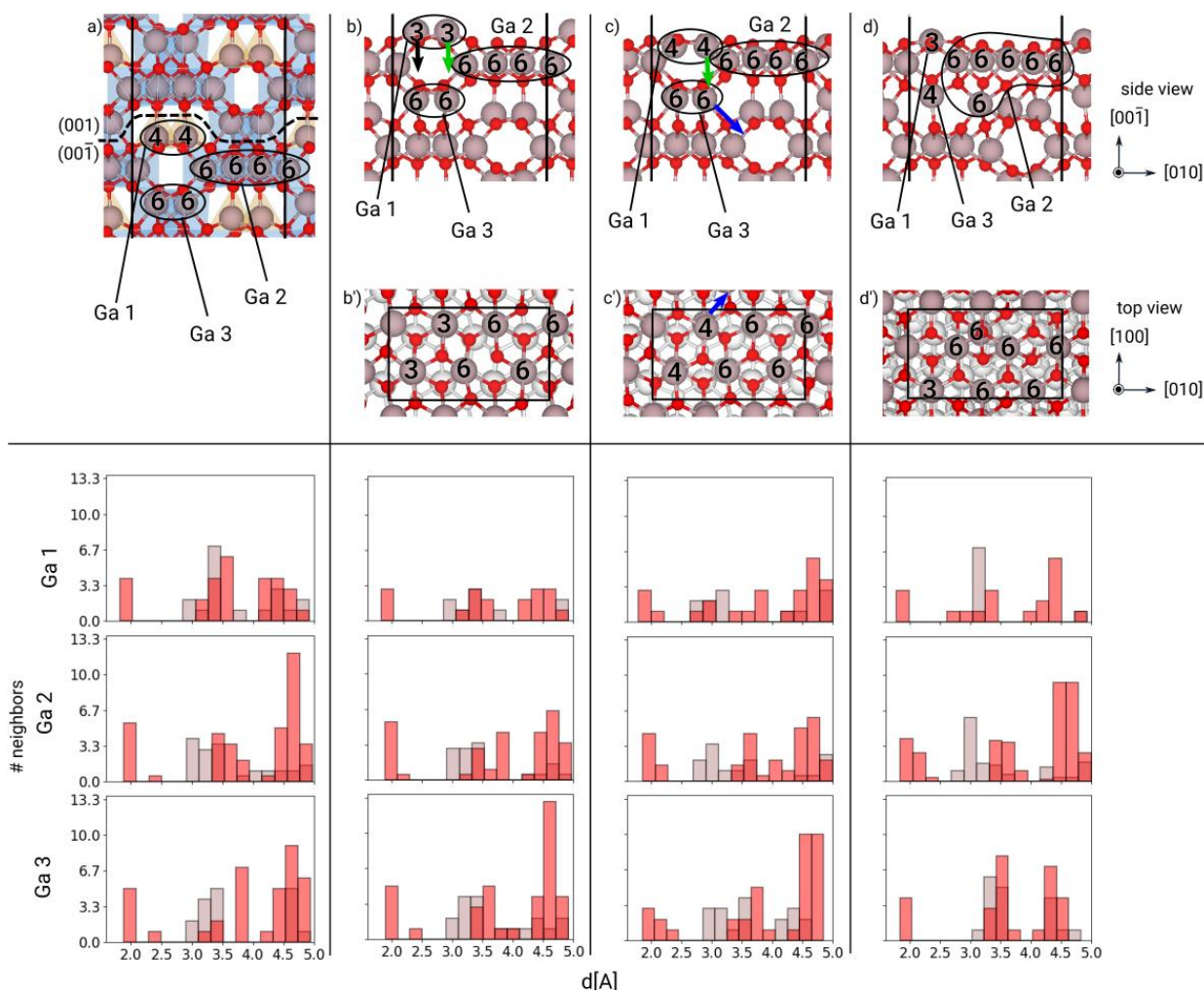


Figure S10: structure (upper panels) and pair distribution function (lower panels) of the slab of the (00-1) surface of κ - Ga_2O_3 at different steps of optimization: (a) bulk, (b-b') "as-cut", (c-c') "relaxed" and (d-d') "reconstructed". In the case of the bulk, the different tetrahedral or octahedral cages are represented through orange or blue polyhedra, respectively. For the atoms closest to the surface, the average number of first neighbors is reported. The most important atomic displacements between one structure and the following are highlighted by black, blue and green arrows. The interatomic distances are shown for selected Ga atoms, labelled "Ga 1", "Ga 2" and "Ga 3".

Additional details about the calculation of the cohesive energies of the misfit-strained bulk of Ga_2O_3 polymorphs and the spontaneous reconstruction of (001) κ - Ga_2O_3 with sapphire misfit strain.

In Figure S11 we report the cohesive energies of the bulk of the different phases of Ga_2O_3 after the application of an anisotropic strain. The bulk unit cells have been constructed in order to be orthorhombic and terminating with its (001) planes exposing the same structure of the β -(-201), α -(001) and κ -(001) surfaces (see Table S3).

We further describe here the optimization process of the {001} κ - Ga_2O_3 thin slab, including 100 atoms, when one of the two terminations, i.e. the (00-1) one, undergoes a spontaneous reconstruction in the case of misfit strain with the Al_2O_3 substrate. Since the overall change in structure affecting also the subsurface region, our goal is to gain some qualitative insight about the reconstruction steps. We inspected the geometries of the complete optimization path, and we identified seven key images of the process: we report their energy and structures in Figure S12.

The evolution of the energy profile of the optimization (Figure S12a) shows a monotone descent towards one minimum, with no barrier. In particular, we began our structural optimization from a structure where we applied an in-plane strain only, without modifying the atomic coordinates along the direction perpendicular to the surface (which we expect to

be relaxed by the optimization). This procedure might have artificially placed the system into a state with such an energy and configuration facilitating the steepest descent towards the reconstructed geometry.

Nonetheless, we can still obtain useful information about the reconstruction of the surface: the step-by-step comparison of the structure of the images suggests that the rearrangement of the atoms might be driven by the strong preference of Ga atoms for an octahedral coordination rather than a tetrahedral one. The whole process requires a two-steps diffusion of two Ga atoms, accompanied by the diffusion of the O atoms nearby, thus providing a rather complex energy landscape.

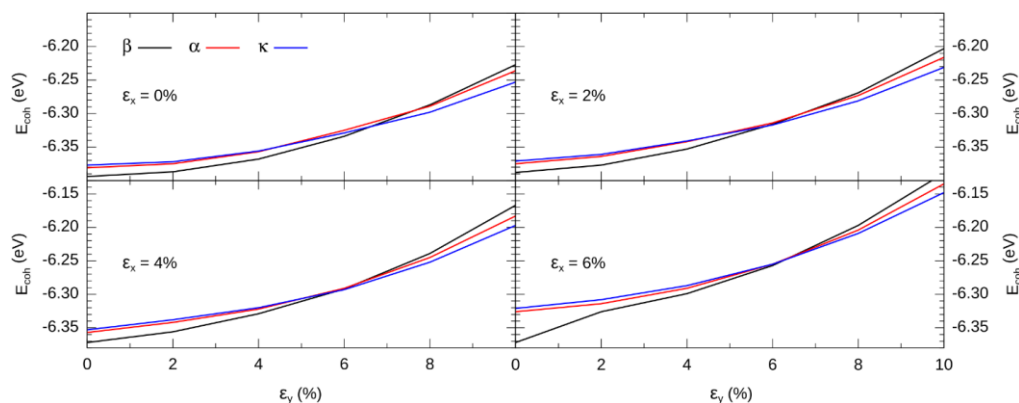


Figure S11: calculation of the cohesive energy E_{coh} in the case of a biaxial strain for the three polymorphs of Ga_2O_3 . The x/y axis is aligned with the $[100]/[-120]$ direction of c-sapphire. In the case of the β -, κ - and α - Ga_2O_3 , these directions correspond to $[-10-2]/[0-10]$, $[100]/[010]$ and $[100]/[-120]$ ones, respectively.

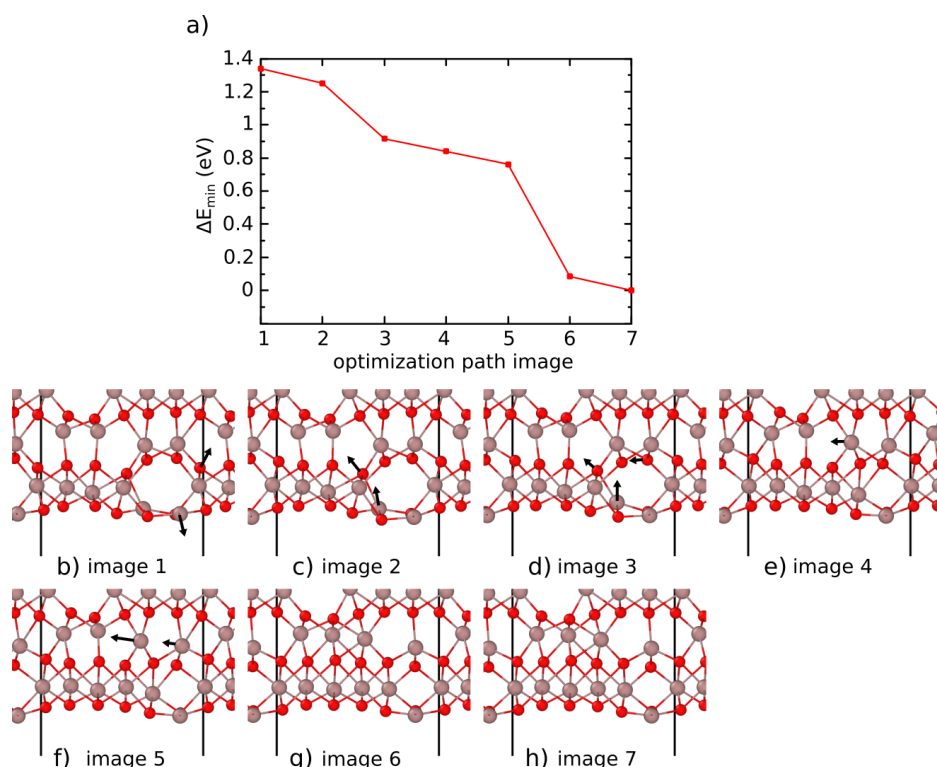


Figure S12: most significant snapshots extracted from the optimization of the $\{001\}$ κ - Ga_2O_3 surface, strained by the misfit with the (001) α - Al_2O_3 substrate. Panel a shows the energy profile of the collection of subsequent images, whose geometry is shown in panels b-h. For each image, a sideview of lower part of the slab, with the $(00-1)$ surface placed at the bottom, is shown. The most important atomic displacements from one step to the following one are marked by black arrows.

References

1. Yu M, Trinkle DR. Accurate and efficient algorithm for Bader charge integration. *J Chem Phys* [Internet]. 2011 Nov;134(6):64111. Available from: <https://doi.org/10.1063/1.3553716>
2. Henkelman G, Arnaldsson A, Jónsson H. A fast and robust algorithm for Bader decomposition of charge density. *Comput Mater Sci* [Internet]. 2006;36(3):354–60. Available from: <https://www.sciencedirect.com/science/article/pii/S0927025605001849>
3. Yoshioka S, Hayashi H, Kuwabara A, Oba F, Matsunaga K, Tanaka I. Structures and energetics of Ga₂O₃ polymorphs. *Journal of Physics: Condensed Matter* [Internet]. 2007 Jul;19(34):346211. Available from: <https://dx.doi.org/10.1088/0953-8984/19/34/346211>
4. Furthmüller J, Bechstedt F. Quasiparticle bands and spectra of Ga₂O₃ polymorphs. *Phys Rev B* [Internet]. 2016 Mar;93(11):115204. Available from: <https://link.aps.org/doi/10.1103/PhysRevB.93.115204>
5. Lipinska-Kalita KE, Kalita PE, Hemmers OA, Hartmann T. Equation of state of gallium oxide to 700.3em0exGPa: Comparison of quasihydrostatic and nonhydrostatic compression. *Phys Rev B* [Internet]. 2008 Mar;77(9):94123. Available from: <https://link.aps.org/doi/10.1103/PhysRevB.77.094123>
6. Hinuma Y, Gake T, Oba F. Band alignment at surfaces and heterointerfaces of Al₂O₃, Ga₂O₃, In₂O₃, and related group-III oxide polymorphs: A first-principles study. *Phys Rev Mater* [Internet]. 2019 Aug;3(8):84605. Available from: <https://link.aps.org/doi/10.1103/PhysRevMaterials.3.084605>
7. Cora I, Mezzadri F, Boschi F, Bosi M, Čaplovičová M, Calestani G, et al. The real structure of ε-Ga₂O₃ and its relation to κ-phase. *CrystEngComm* [Internet]. 2017;19(11):1509–16. Available from: <http://dx.doi.org/10.1039/C7CE00123A>
8. Stuart NM, Sohlberg K. A method of calculating surface energies for asymmetric slab models. *Phys Chem Chem Phys* [Internet]. 2023;25(19):13351–8. Available from: <http://dx.doi.org/10.1039/D2CP04460A>
9. Hinuma Y, Kamachi T, Hamamoto N, Takao M, Toyao T, Shimizu K ichi. Surface Oxygen Vacancy Formation Energy Calculations in 34 Orientations of β-Ga₂O₃ and θ-Al₂O₃. *The Journal of Physical Chemistry C* [Internet]. 2020;124(19):10509–22. Available from: <https://doi.org/10.1021/acs.jpcc.0c00994>
10. Zhou X, Hensen EJM, van Santen RA, Li C. DFT Simulations of Water Adsorption and Activation on Low-Index α-Ga₂O₃ Surfaces. *Chemistry – A European Journal* [Internet]. 2014;20(23):6915–26. Available from: <https://chemistry-europe.onlinelibrary.wiley.com/doi/abs/10.1002/chem.201400006>
11. Lucht M, Lerche M, Wille HC, Shvyd'ko Yu V, Rüter HD, Gerdau E, et al. Precise measurement of the lattice parameters of α-Al₂O₃ in the temperature range 4.5–250K using the Mössbauer wavelength standard. *J Appl Crystallogr* [Internet]. 2003 Aug;36(4):1075–81. Available from: <https://doi.org/10.1107/S0021889803011051>